Supplementary Materials

Subcompositional dominance and distances

We consider the central log-ratio transformation in order to pursue our analysis without considering both the block effect and residuals for the more integrated traits and residuals for protein abundances. We are aloud to do so since the clr-transformation satisfies the subcompositional dominance property, *i.e.*, for each couple of vectors, $\boldsymbol{x}$ and $\boldsymbol{y}$, and for each pair of subvectors $\hat{\boldsymbol{x}}$ and $\hat{\boldsymbol{y}}$ of $\boldsymbol{x}$ and $\boldsymbol{y}$, respectively, obtained by selecting the same set of components, the distance between the subvectors is always less than or equal to the distance between the original vectors, *i.e.*

$$d(\boldsymbol{x},\boldsymbol{y}) \geq d(\hat{\boldsymbol{x}},\hat{\boldsymbol{y}}) \tag{S1}$$

Therefore, for each $\boldsymbol{z}$ such that $d(\boldsymbol{x},\boldsymbol{y}) \geq d(\boldsymbol{x},\boldsymbol{z})$, we have that, dividing eq.(S1) by $\frac{d(\boldsymbol{x},\boldsymbol{z})}{d(\hat{\boldsymbol{x}},\hat{\boldsymbol{z}})} \geq 1$

$$\alpha d(\hat{\boldsymbol{x}},\hat{\boldsymbol{z}}) \geq k d(\hat{\boldsymbol{x}},\hat{\boldsymbol{y}}) \tag{S2}$$

where $\alpha = \frac{d(\boldsymbol{x},\boldsymbol{y})}{d(\boldsymbol{x},\boldsymbol{z})} \geq 1$ and $k = \frac{d(\hat{\boldsymbol{x}},\hat{\boldsymbol{z}})}{d(\boldsymbol{x},\boldsymbol{z})} \leq 1$. So, since $k/\alpha \leq 1$

$$d(\hat{\boldsymbol{x}},\hat{\boldsymbol{y}}) \geq d(\hat{\boldsymbol{x}},\hat{\boldsymbol{z}}) \tag{S3}$$

As a consequence, distance relationship between the original vectors is preserved by selected subvectors.

The fitting algorithm

The hglm package implements the estimation algorithm for hierarchical generalized linear models. It fits generalized linear models with random effects, where the random effect may come from a conjugate exponential-family distribution (Gaussian, Gamma, Beta or inverse-Gamma) and it is possible to explicitly specify the design matrices both for the fixed and random effects, which allows fitting correlated random effects as well as random regression models.
In order to perform the diallel analysis, we considered $\mathbf{y}$, the vector of observations for the trait of interest, and we re-wrote the model (eq.(2)) in matrix a form:

$$\boldsymbol{y} = X\boldsymbol{\beta} + Z\boldsymbol{u} + \boldsymbol{\epsilon} \tag{S4}$$

where X is the design matrix for the fixed effects, Z the design matrix for the random effects, $\boldsymbol{\beta} = (\mu, \beta_{S.uvarum}, \beta_{S.cerevisiae})$ and $\boldsymbol{u} = (\boldsymbol{A_w}, \boldsymbol{A_b}, \boldsymbol{B}, \boldsymbol{H_w}, \boldsymbol{H_b})$ are respectively the vectors of fixed effects parameters and random effects parameters, and $\boldsymbol{\epsilon}$ is the vector of random errors. With this notation, the construction of the model is straight forward since we just have to construct the design matrices for both fixed and random effects.

Let n be the number of observations, J the total number of parental strains, N_{intra} (resp. N_{inter}) the number of intra-specific (resp. inter-specific) crosses, and K the total number of random effects parameters. X is a $n \times 3$ matrix, with, by construction, the first column equal to $(1, 1, ..., 1)$, while the elements of the second and third columns (for respectively *S. uvarum* and *S. cerevisiae*) are 1 or 0 depending on whether the strain is inbred and or not.
Z will be a $n \times K$ matrix and, more precisely, it can be thought as the following block matrix:

$$Z = \left[\begin{array}{c:c:c:c:c} & & & & \\ Z_{\boldsymbol{A_w}} & Z_{\boldsymbol{A_b}} & Z_{\boldsymbol{B}} & Z_{\boldsymbol{H_w}} & Z_{\boldsymbol{H_w}} \\ & & & & \end{array}\right] \tag{S5}$$

where $Z_{\boldsymbol{A_w}}$, $Z_{\boldsymbol{A_b}}$, $Z_{\boldsymbol{B}}$, $Z_{\boldsymbol{H_w}}$, $Z_{\boldsymbol{H_b}}$ denote the design matrices, respectively, of the random effect parameters $\boldsymbol{A_w}$, $\boldsymbol{A_b}$, $\boldsymbol{B}$, $\boldsymbol{H_w}$ and $\boldsymbol{H_b}$. In particular, $Z_{\boldsymbol{A_w}}$, $Z_{\boldsymbol{A_b}}$, $Z_{\boldsymbol{B}}$ are $n \times J$ matrices, $Z_{\boldsymbol{H_w}}$ is a $n \times N_{intra}$ matrix and $Z_{\boldsymbol{H_b}}$ is a $n \times N_{inter}$ matrix with entries:

$$z_{\boldsymbol{A_{w_{ij}}}} = \begin{cases} 2 & \text{If the } i\text{-observation belongs to a parental strain, the } j\text{-th;} \\ 1 & \text{If the } i\text{-observation belongs to an hybrid achieved through an intra- specific cross} \\ & \text{in which the parental strain } j \text{ is involved;} \\ 0 & \text{otherwise;} \end{cases} \tag{S6}$$

$$z_{\boldsymbol{A_{b_{ij}}}} = \begin{cases} 1 & \text{If the } i\text{-observation belongs to an hybrid achieved through an inter- specific cross} \\ & \text{in which the parental strain } j \text{ is involved;} \\ 0 & \text{otherwise;} \end{cases} \tag{S7}$$

$$z_{\boldsymbol{B_{ij}}} = \begin{cases} 1 & \text{If the } i\text{-observation belongs to a parental strain, the } j\text{-th;} \\ 0 & \text{otherwise;} \end{cases} \tag{S8}$$

and, enumerating the intra-specific/inter-specific hybrid strains with k_{intra}/k_{inter} from 1 to N_{intra}/N_{inter}, respectively,

$$z_{\boldsymbol{H_{w_{ik_{intra}}}}} = \begin{cases} 1 & \text{If the } i\text{-observation belongs to the } k_{intra}\text{- hybrid strain;} \\ 0 & \text{otherwise;} \end{cases} \tag{S9}$$

$$z_{\boldsymbol{H_{b_{ik_{inter}}}}} = \begin{cases} 1 & \text{If the } i\text{-observation belongs to the } k_{inter}\text{- hybrid strain;} \\ 0 & \text{otherwise;} \end{cases} \tag{S10}$$

Half-diallel simulation construction

In order to elucidate our findings about the decoupling of inbreeding and heterotic variances, we simulated a half-diallel between N parental strains. We supposed the phenotypic values of each trait to depend on a fixed number of loci, L, and we considered all the possible combinations of genetic effects, namely presence/absence of dominance, of additive $\times$ additive epistasis and of additive $\times$ additive epistasis.
We let the number of alleles at each locus to vary between 1 and N and we drew values for allele a at locus i (a_i) from a Gamma distribution ($\Gamma(k,\theta)$), for additive $\times$ additive epistatic effect between a_i and a_j (aa^{ij}) and for dominance $\times$ dominance epistatic effect (dd^{ij}) from a Gaussian distribution ($\mathcal{N}(0,\sigma^2)$). The dominance effect between alleles a and b at locus i (d^i_{ab}) are drawn from an uniform distribution $\mathcal{U}(0,m)$ with $m = 0.5$ for dominance of the strongest allele, and $m = 1$ for symmetrical dominance. Therefore, the phenotypic value of the parental lines P_k and of the hybrid, H_{lk}, between parents P_k and P_l are given by:

1) Additive model

$$y_{P_k} = 2\sum_i k_i\,, \quad y_{H_{lk}} = \sum_i k_i + \sum_i l_i \tag{S11}$$

2) Additive model plus dominance

$$y_{P_k} = 2\sum_i k_i\,, \quad y_{H_{lk}} = \sum_i k_i + \sum_i l_i + \sum_i d^i_{kl} \tag{S12}$$

3) Additive model plus *additive* $\times$ *additive* effect

$$y_{P_k} = 2\sum_i k_i + \sum_{ij} aa^{ij}\,, \quad y_{H_{lk}} = \sum_i k_i + \sum_i l_i \tag{S13}$$

4) Additive model plus *dominance* $\times$ *dominance* effect

$$y_{P_k} = 2\sum_i k_i\,, \quad y_{H_{lk}} = \sum_i k_i + \sum_i l_i + \sum_{ij} dd^{ij} \tag{S14}$$

5) Additive model plus *additive* $\times$ *additive* and *dominance* $\times$ *dominance* effect

$$y_{P_k} = 2\sum_i k_i + \sum_{ij} aa^{ij}\,, \quad y_{H_{lk}} = \sum_i k_i + \sum_i l_i + \sum_{ij} dd^{ij} \tag{S15}$$

6) Additive model plus dominance and *additive* $\times$ *additive* effect

$$y_{P_k} = 2\sum_i k_i + \sum_{ij} aa^{ij}\,, \quad y_{H_{lk}} = \sum_i k_i + \sum_i l_i + \sum_i d^i_{kl} \tag{S16}$$

7) Additive model plus dominance and *dominance* $\times$ *dominance* effect

$$y_{P_k} = 2\sum_i k_i\,, \quad y_{H_{lk}} = \sum_i k_i + \sum_i l_i + \sum_i d^i_{kl} + \sum_{ij} dd^{ij} \tag{S17}$$

8) Additive model plus dominance, *additive* $\times$ *additive* and *dominance* $\times$ *dominance* effect

$$y_{P_k} = 2\sum_i k_i + \sum_{ij} aa^{ij}\,, \quad y_{H_{lk}} = \sum_i k_i + \sum_i l_i + \sum_i d^i_{kl} + \sum_{ij} dd^{ij} \tag{S18}$$

Inbreeding depression and heterosis variances are equal in three-parent diallel

Inbreeding and heterosis variances are equal in the particular case of a three-parent diallel when no maternal effect is present. It can be easily seen by the direct computation of their value.
In order to do that we decompose the phenotypic values of the $i-$parent, P_i, as

$$P^d_i = \mu + 2A_i \tag{S19}$$

and of the $i \times j$ hybrid, H_{ij}, as

$$H^d_{ij} = \mu + A_i + A_j \tag{S20}$$

where $\mu = \frac{1}{6}(P_1 + P_2 + P_3 + H_{12} + H_{13} + H_{23})$ is the mean phenotypic value of the population and

$$A_i = \frac{1}{3}(P_i + \sum_{j\neq i} H_{ij}) - \mu \tag{S21}$$

the GCA of strain i. Therefore, we can express the inbreeding depression variance as the deviation of the decomposed phenotypic value of the parents, P^d, and their true value P

$$Var(inbreeding) = \frac{1}{3}\sum_i (P^d_i - P_i - (\overline{P^d - P}))^2 \tag{S22}$$

and the heterosis variance analogously

$$Var(heterosis) = \frac{1}{3}\sum_{i<j}(H_{ij}^{d} - H_{ij} - (\overline{H^{d} - H}))^2 \tag{S23}$$

In which we have used the fact that $H_{ij} = H_{ji}$, since no maternal effects are present.

Substituting S19 and S21 in S22, we get

$$\begin{aligned}
Var(inbreeding) &= \frac{1}{3}\sum_{i=1}^{3}(\mu + 2A_i - P_i - \frac{1}{3}\sum_{k=1}^{3}(\mu + 2A_k - P_k))^2 = \\
&= \frac{1}{3}\sum_{i=1}^{3}(\mu + \frac{2}{3}(P_i + \sum_{j\neq i} H_{ij}) - 2\mu - P_i - \frac{1}{3}\sum_{k=1}^{3}(\mu + \frac{2}{3}(P_k + \sum_{j\neq k} H_{kj}) - 2\mu - P_k))^2 = \\
&= \frac{1}{243}\sum_{i=1}^{3}(6P_i + 6\sum_{j\neq i} H_{ij} - 9\mu - 9P_i - \sum_{k=1}^{3}(2P_k + 2\sum_{j\neq k} H_{kj} - 3\mu - 3P_k))^2 = \\
&= \frac{1}{243}\sum_{i=1}^{3}(6\sum_{j\neq i} H_{ij} - 9\mu - 3P_i + \sum_{k=1}^{3} P_k - 4\sum_{j<k} H_{kj} + 9\mu)^2 = \\
&= \frac{1}{243}\sum_{i=1}^{3}(-2P_i + P_j + P_k + 2H_{ik} + 2H_{ij} - 4H_{kj})^2
\end{aligned} \tag{S24}$$

where $i \neq j \neq k$. In the same way, substituting S20 and S21 in S23, we get

$$\begin{aligned}
Var(heterosis) &= \frac{1}{3}\sum_{i<j}(\mu + A_i + A_j - H_{ij} - \frac{1}{3}\sum_{k<m}(\mu + A_k + A_m - H_{km}))^2 = \\
&= \frac{1}{3}\sum_{i<j}(\frac{1}{3}(P_i + P_j + \sum_{k\neq i} H_{ik} + \sum_{k\neq j} H_{jk}) - \mu - H_{ij} - \frac{1}{3}\sum_{k<m}(\frac{1}{3}(P_k + P_m + \sum_{l\neq k} H_{kl} + \sum_{l\neq m} H_{ml}) - \mu - H_{km}))^2 = \\
&= \frac{1}{243}\sum_{i<j}(3(P_i + P_j + \sum_{k\neq i} H_{ik} + \sum_{k\neq j} H_{jk}) - 9\mu - 9H_{ij} - (2\sum_{k} P_k + \sum_{k<m} H_{km} - 9\mu))^2 = \\
&= \frac{1}{243}\sum_{i<j}(3(P_i + P_j + \sum_{k\neq i} H_{ik} + \sum_{k\neq j} H_{jk}) - 9H_{ij} - 2\sum_{k} P_k - \sum_{k<m} H_{km})^2 = \\
&= \frac{1}{243}\sum_{i<j}(P_i + P_j - 2P_k - 4H_{ij} + 2H_{ik} + 2H_{jk})^2
\end{aligned} \tag{S25}$$

where again $i \neq k \neq j$. Therefore,

$$\begin{aligned}
Var(inbreeding) &= \frac{1}{243}\sum_{i=1}^{3}(-2P_i + P_j + P_k + 2H_{ik} + 2H_{ij} - 4H_{kj})^2 = \\
&= \frac{1}{243}((-2P_1 + P_2 + P_3 + 2H_{12} + 2H_{13} - 4H_{23})^2 + (-2P_2 + P_1 + P_3 + 2H_{12} + 2H_{23} - 4H_{13})^2 + \\
&+ (-2P_3 + P_1 + P_2 + 2H_{13} + 2H_{23} - 4H_{12})^2 = \frac{1}{243}\sum_{i<j}(-2P_k + P_i + P_j + 2H_{ik} + 2H_{jk} - 4H_{ij})^2 = Var(heterosis)
\end{aligned} \tag{S26}$$

Structuration of genetic variability at the fermentation trait level

A Gaussian mixture model is run to classify life-history and fermentation traits according to their genetic variance components.

The best model clearly identify three clusters (fig.SF3 and fig.SF6). Cluster 1 (99.9% of good assignments) is composed by 9 traits, characterized by having null inter-specific additive variance component, relatively low inter-specific heterosis variance and high intra-specific additive and inbreeding components. In this cluster we can find most volatile compounds such as *Octanoic acid* and *Hexanol* at both temperatures, *Phenyl-2-ethanol*, *Phenyl-2-ethanol acetate* and *Decanoic acid* at 18°C, the kinetic parameter CO_{2max} and the life-history trait *Size-t-*N_{max} at 26°C. Cluster 2 (98.9% of good assignments) consists of 28 traits that are characterized by high inter-specific additive and inbreeding components ($\sigma^2_{\boldsymbol{A_b}}$ and $\sigma^2_{\boldsymbol{B}}$), relatively low heterosis ($\sigma^2_{\boldsymbol{H_w}}$ and $\sigma^2_{\boldsymbol{H_b}}$) and intra-specific additive variances ($\sigma^2_{\boldsymbol{A_w}}$). Most kinetic parameters and life-history traits belongs to this cluster: *t-lag*, V_{max}, *t-45*, *r*, *t-*N_{max}, J_{max} and *Viability-t-*N_{max} at both temperatures; *t-*V_{max} and *t-75* at 26°C; *AFtime*, *t-*N_0, *Size-t-*N_{max} at 18°C. We can also find some basic enological parameters and aromatic traits - *Isoamyl acetate* and *Hexanoic acid* at both temperatures; *Phenyl-2-ethanol* and *Phenyl-2-ethanol acetate* at 26°C; *X4MMP*, *Free* SO_2 and *Total* SO_2 at 18°C. Traits attributed to cluster 3 (19 traits, 97.3% of good assignments) have high additive and heterotic variances and null inbreeding variance. The rest of the basic enological parameters and aromatic traits along with some kinetics parameters and life-history traits belongs to it.

As for protein abundances, we choose to consider life-history and fermentation traits at two temperatures (18°C and 26°C) as different traits. Indeed, after computation of genetic variance components for each trait, correlations between temperatures are not found to be significant except for 6 traits ($t\text{-}V_{max}$, *t-45*, *r*, $t\text{-}N_{max}$, *Viability-t-*N_{max} and *Hexanol*) that are highly and positively correlated. All of them fall in the same cluster at the two temperatures, except $t\text{-}V_{max}$. Overall, we find that 79% of traits do not belong to the same cluster at the two temperatures. Further, Pearson's correlation tests are performed to investigate the correlation between genetic effects at the two temperatures. They were not significant except for the additive inter-specific component ($cor = 0.74$, p-value<0.05). Therefore, at the fermentation trait level, genotype by environment interactions predominate.

Globally, correlations between variance components, when present, are found to be negative (fig.SF4). However, the pattern changes when considering intra-group correlations. Indeed, in cluster 2, even if inbreeding is negatively correlated to the heterotic variances, it is positively correlated to the additive inter-specific variance, and in cluster 3, additive genetic variances are positively correlated to each other. In cluster 1, there is no statistical significant correlation between genetic effects (fig.SF7).

Therefore, we can state that three well defined groups of traits can be differentiated according to their genetic variance profiles and we show that the part of phenotypic variation explained by the model's parameters depends on trait's category and temperature: in cluster 1, we can find mostly aromatic traits; in cluster 2 kinetics parameters and life-history traits and in cluster 3 most enological parameters. Further, closely related phenotypes show similar profiles in terms of variance components, such as CO_{2max}, *Ethanol* and *Residual Sugar* that clusters together at 18°C; *Total* SO_2 and *Free* SO_2 are found in cluster 2 at 18°C and in cluster 3 at 26°C; $t\text{-}N_0$ and *t-lag* in cluster 2 at 18°C. We finally see that inbreeding variance can be either negatively, or not correlated to heterotic effects.

Strain characterization

We characterized the strains based on their genetic contribution to the total phenotypic value of a trait at a certain temperature (fig. SF11). Strain D1 is found to be the strain with the lowest additive contribution for *Phenyl-2-ethanol* at both temperatures and for *Sugar.Ethanol.Yield* (except in inter-specific crosses at 18°C), with the highest additive intra-specific contribution for *Decanoic* and *Octanoic acid*, while displaying the highest heterosis contribution for *Octanoic acid* when crossed with E2 at 18°C, with E5 and U1 at 26°C, and for *Decanoic acid* when crossed with E4 at 26°C and U2 at 18°C. D2 and E2 strains have the highest or lowest additive contributions across almost all traits, mostly fermentation kinetics parameters and life history traits. In particular, D2 strain shows the highest intra- and inter-specific additive effects, and inbreeding values for *t.45*, *t.75* and *AFtime* at both temperatures, where the highest heterosis effect is achieved when crossed with E2, U1 for *t*.45 at 18°C, with E5 and U1 for *t*.75 with the first at both temperatures and the latter at 18°C. Similarly, the additive intra-specific effect of U4 is the highest or the lowest for almost all aromatic traits at 18°C (higher for *Phenyl-2-ethanol, Hexanol* and *Hexanoic acid*; lowest for *Decanoic acid* and *Octanoic acid*). Strain U1 shows the highest additive inter-specific effect in aromatic traits at 26°C (*Phenyl-2-ethanol, Phenyl-2-ethanol acetate, Hexanol, Hexanoic acid* and *Octanoic acid*). In particular, the heterosis effect in the inter-specific cross with strain D2 is the highest for *Hexanol* and with strain E2 for *Phenyl-2-ethanol*. For all traits, E5 produces intermediate heterosis values when crossed with E2, E3, E4, W1, U1 and U4 at 18°C, but its cross with E4 results in the highest heterosis value for $t.N_{max}$, and the lowest for *Decanoic acid* with E3 and for *Total* SO_2 with W1 at 26°C. In the same way, crosses between E3 and U1, U2 or U3, between E4 and U1 or W1 never show extreme heterosis values for any trait.

Supplementary tables

Table ST3 Diallel table representing the mitochondrial inheritance for each phenotyped cross: the data clearly shows too many *unknown*s to enter a mitochondrial effect in the model. Backslashes indicate the not phenotyped reciprocals.

P1\ P2	**D1**	**D2**	**E2**	**E3**	**E4**	**E5**	**W1**	**U1**	**U2**	**U3**	**U4**
D1	D1	D2	unknown	\	unknown	\	unknown	\	U2	U3	U4
D2	\	D2	E2	\	E4	\	W1	\	\	\	\
E2	\	\	E2	unknown	unknown	E5	unknown	\	U2	U3	U4
E3	D1	D2	\	E3	unknown	\	W1	\	U2	U3	\
E4	\	\	\	\	E4	E5	W1	U1	U2	U3	U4
E5	D1	unknown	\	unknown	\	E5	unknown	U1	U2	U3	\
W1	\	\	\	\	\	\	W1	\	U2	U3	\
U1	D1	D2	E2	E3	\	\	CW1	U1	\	\	\
U2	\	D2	\	\	\	\	\	unknown	U2	\	\
U3	\	D2	\	\	\	\	\	unknown	unknown	U3	\
U4	\	unknown	\	E3	\	E5	W1	unknown	unknown	unknown	U4

Table ST4 Pearson's chi-square. For each cluster and at each temperature (18° and 26°) we tested for enrichment in proteins belonging to a certain functional category using as prior probability the frequency of proteins functional category based on MIPS database. In yellow (resp. pink) are highlighted the functional category enhanced (resp. depleted) for each cluster and at each temperature when the statistical test was significant.

Cluster	T	P-val	Metabolism (other)	Amino acid metabolism	Nucleotide metabolism	Carbon metabolism	Replication	Transcription	Protein synthesis	Protein fate	Transport	Stress	Mating	Signal	Unknown
1	18	0.873	-0.092	0.592	-0.580	0.296	-0.637	-0.845	0.859	1.091	1.214	-0.591	-0.880	-0.456	-1.021
1	26	0.000	-1.853	-0.053	-0.230	-1.990	-1.102	2.009	-2.702	-2.022	-1.458	10.183	5.900	0.446	-2.336
2	18	0.000	-0.468	3.799	0.519	3.424	-1.970	-1.784	-1.269	3.335	-2.024	2.721	-2.322	-1.409	-2.094
2	26	0.000	-0.431	3.850	0.543	3.477	-1.425	-1.764	-1.235	2.697	-2.000	2.186	-2.303	0.061	-2.425
3	18	0.042	-0.062	2.012	2.550	1.332	-1.239	-0.327	-1.193	-0.387	-1.379	1.564	0.829	-0.886	-1.421
3	26	0.001	0.428	-0.053	1.100	-0.199	-1.102	-1.319	-0.466	3.951	-1.458	2.989	-1.447	0.446	-1.929
4	18	0.026	-0.532	3.519	0.755	-1.109	-1.220	-0.283	0.424	1.345	-1.341	1.622	-0.397	-0.873	-1.383
4	26	0.001	-0.206	2.549	0.301	-1.490	-0.691	-0.175	-0.319	1.483	-1.747	4.180	-0.864	0.989	-1.793
5	18	0.001	2.239	2.060	3.638	0.219	-1.393	-1.262	2.081	-1.803	-1.685	-0.488	-1.359	0.031	-1.731
5	26	0.001	2.063	2.300	2.324	-0.165	-1.645	-2.067	2.744	-0.319	-0.712	-0.931	-1.107	-0.856	-2.440
6	18	0.008	-2.145	0.044	2.562	1.287	-1.048	-1.243	3.483	0.101	-0.943	-0.882	-0.900	0.515	-0.596
6	26	0.118	-1.933	0.855	2.056	1.939	-0.617	-0.642	1.237	-0.284	-0.114	0.350	-1.330	1.094	-1.193
7	18	0.000	0.891	6.649	-1.135	4.290	-1.673	-3.194	1.885	-0.304	-2.198	1.672	-1.634	-2.007	-3.807
7	26	0.000	1.379	7.162	-0.865	5.001	-1.397	-3.095	1.398	-1.032	-2.895	1.776	-1.220	-2.237	-4.176
8	18	0.000	-3.121	-2.200	2.324	-2.679	-1.645	0.603	-2.935	7.348	-2.367	7.463	3.682	-0.186	-3.093
8	26	0.000	-2.899	-2.046	2.651	-2.506	-1.510	0.529	-2.693	5.751	-2.143	7.516	4.186	-0.743	-2.902
9	18	0.000	-1.884	-0.085	-0.252	-1.568	-1.120	1.959	-2.728	-2.050	-1.488	10.081	5.819	0.424	-2.360
9	26	0.013	-1.032	1.433	2.002	-0.882	-0.643	2.830	-1.584	-0.824	2.372	-0.488	-0.230	0.031	-1.731

Supplementary figures

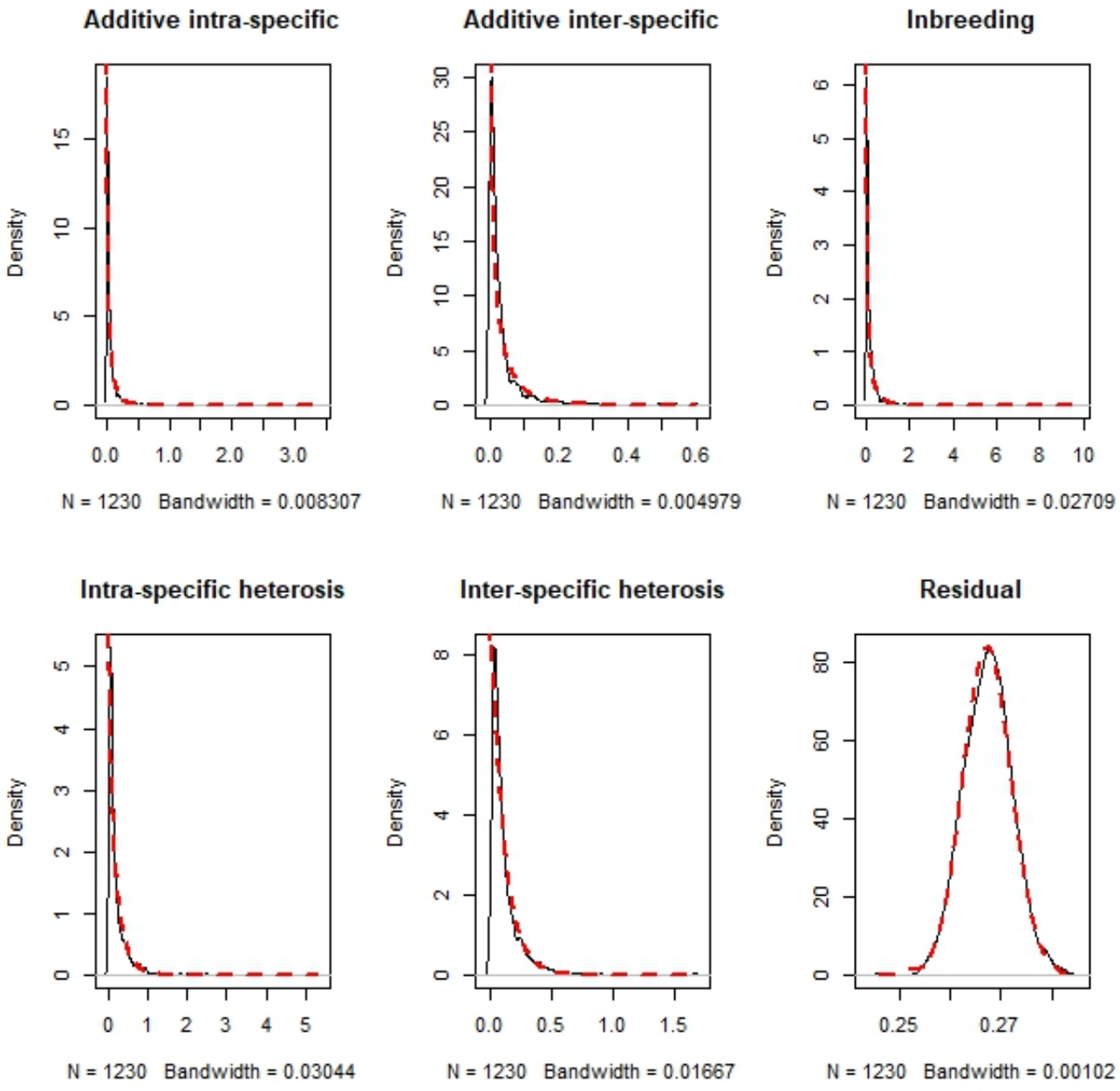

Figure SF1 Density of the variance components estimated by the *hglm* algorithm for the 1230 proteins. Red dashed lines represent the fitted distributions used to simulate and test parameter inference of the proposed model.

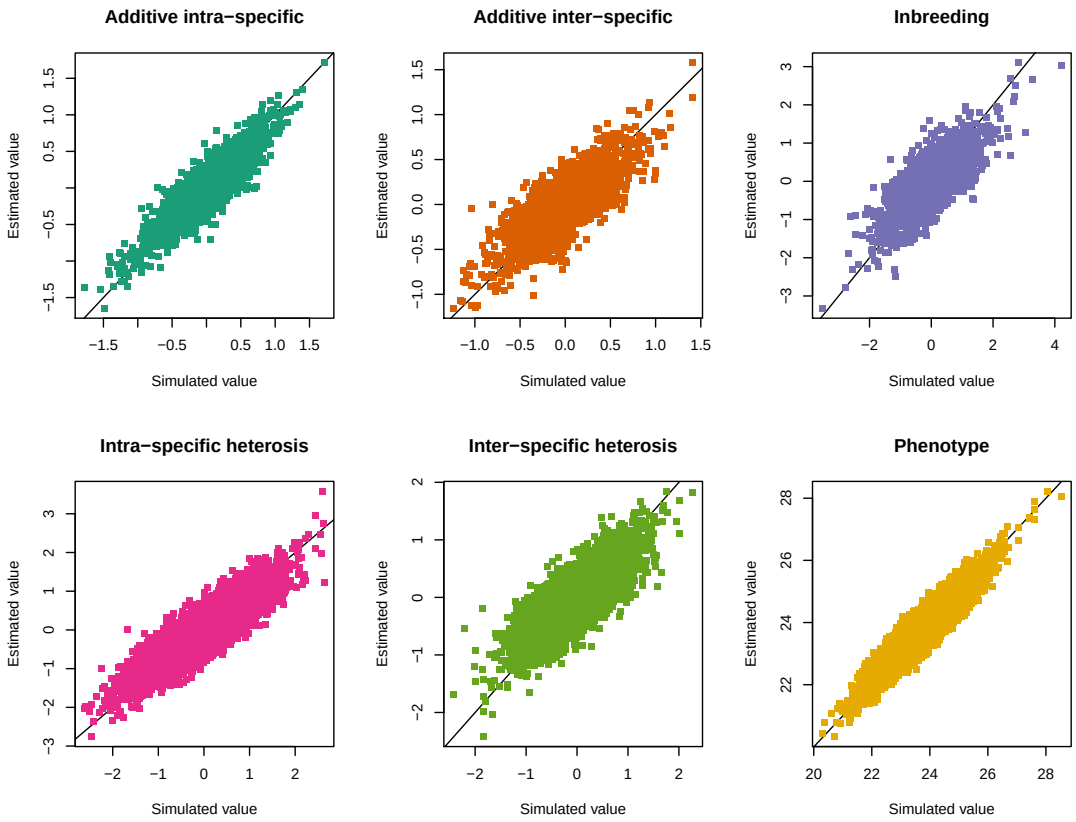

Figure SF2 Fitted Best Linear Unbiased Predictors of the random effects parameters and predicted phenotypic value plotted against the simulated genetic parameters and the simulated phenotypic value. Fixed the number of parental strains and the number of individuals of each species, we performed the simulation 1000 times. Here, we show the case of eleven parents, with 7 belonging to one specie and 4 to the other.

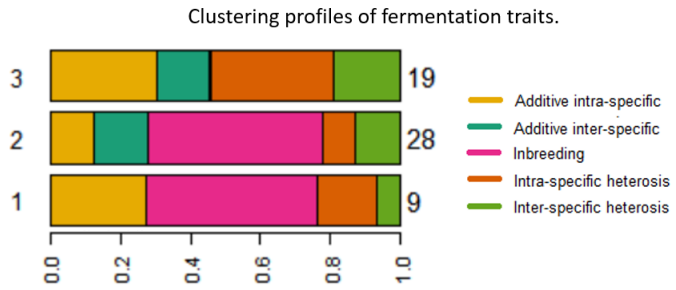

Figure SF3 Clustering profiles of fermentation and life-history traits. Clusters number are reported on the left, on the right the number of traits found in each cluster.

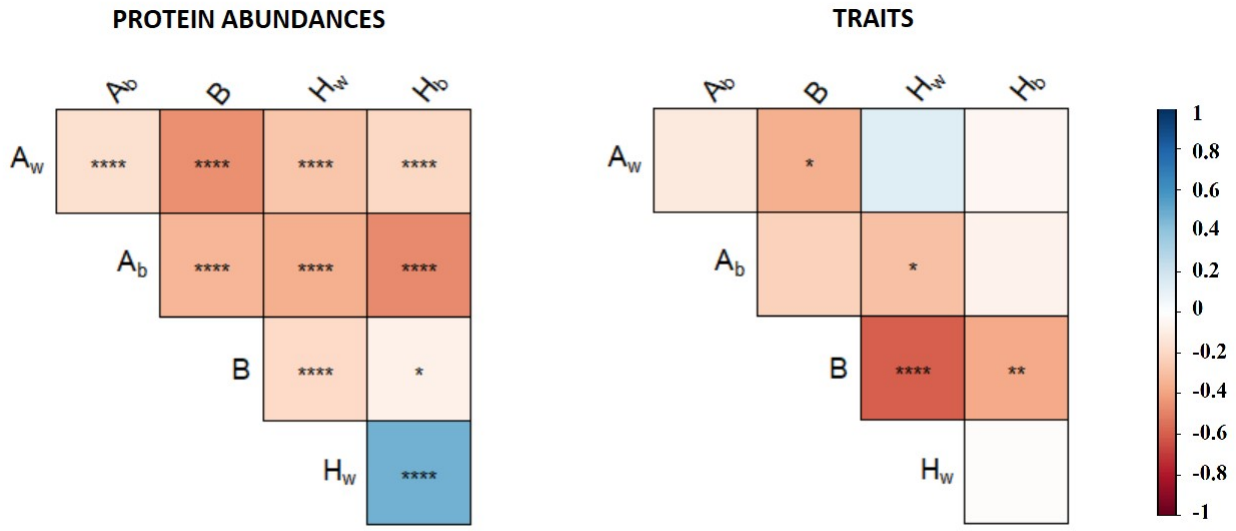

Figure SF4 Global correlations between genetic variance components: on the left correlations at the proteomic level, on the right at the more integrated level. * significant at $p < 0.05$; ** significant at $p < 5 \cdot 10^{-3}$; *** significant at $p < 5 \cdot 10^{-4}$; **** significant at $p < 5 \cdot 10^{-5}$. No symbol: not significant.

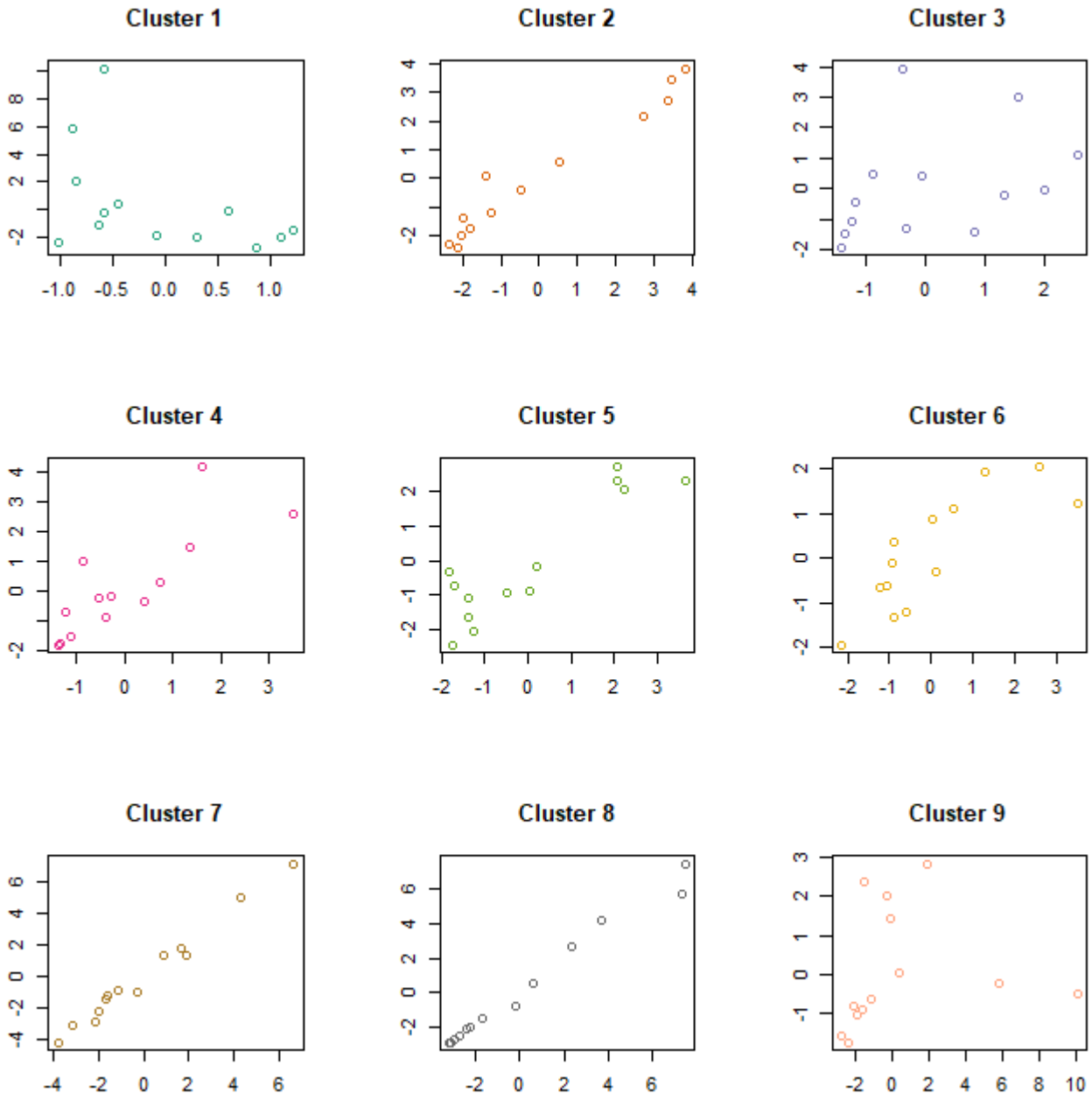

Figure SF5 Pearson's chi-square test of enrichment: For each cluster are represented the chi-square standardized residuals at 18° (abscissa) and at 26° (ordinate).

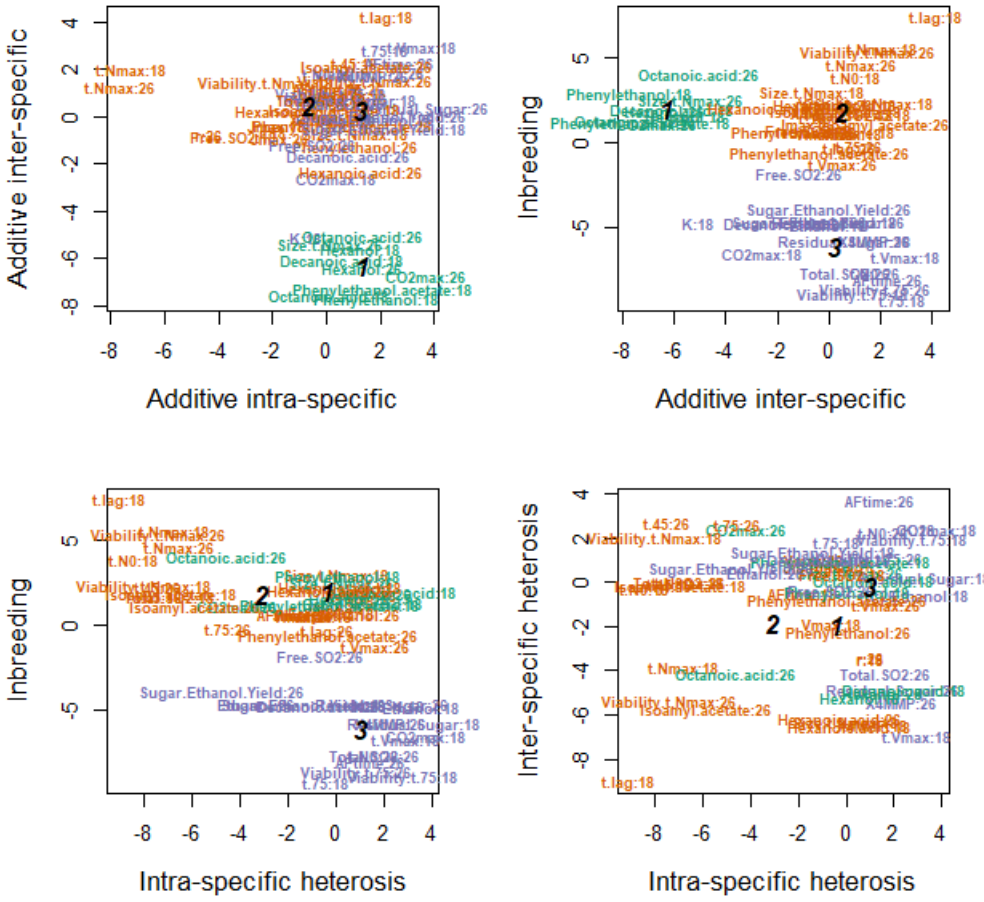

Figure SF6 Life-history and fermentation traits profiles. Traits are identified by their label, color combinations identify the clusters obtained by their classification based on a Gaussian Mixture model.

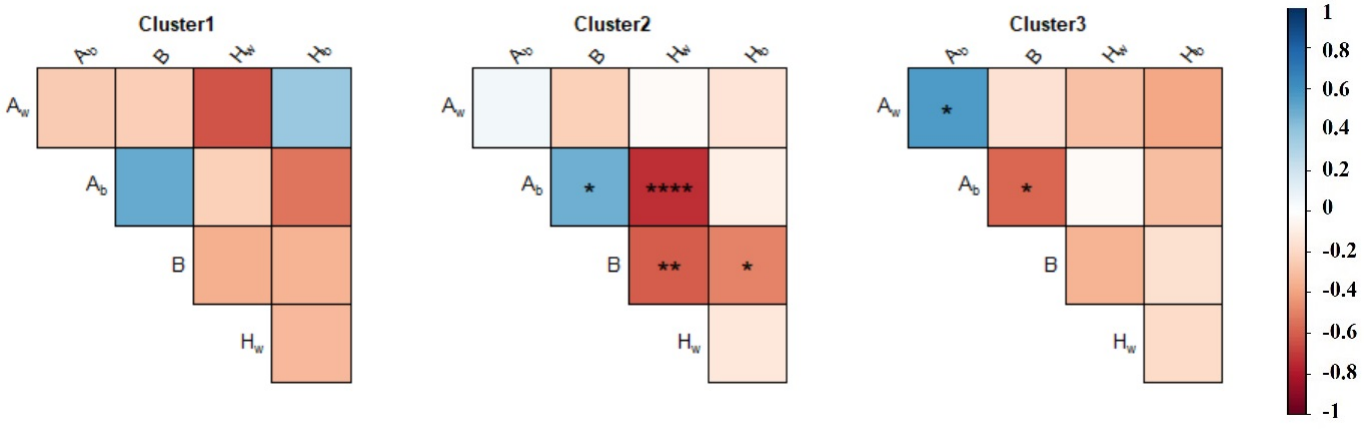

Figure SF7 Pearson's correlation test performed to investigate the intra-cluster correlations at the trait level: for each cluster, the figure shows the correlation between variances of the genetic effects. * significant at $p < 0.05$; ** significant at $p < 5 \cdot 10^{-3}$; *** significant at $p < 5 \cdot 10^{-4}$; **** significant at $p < 5 \cdot 10^{-5}$. No symbol: not significant.

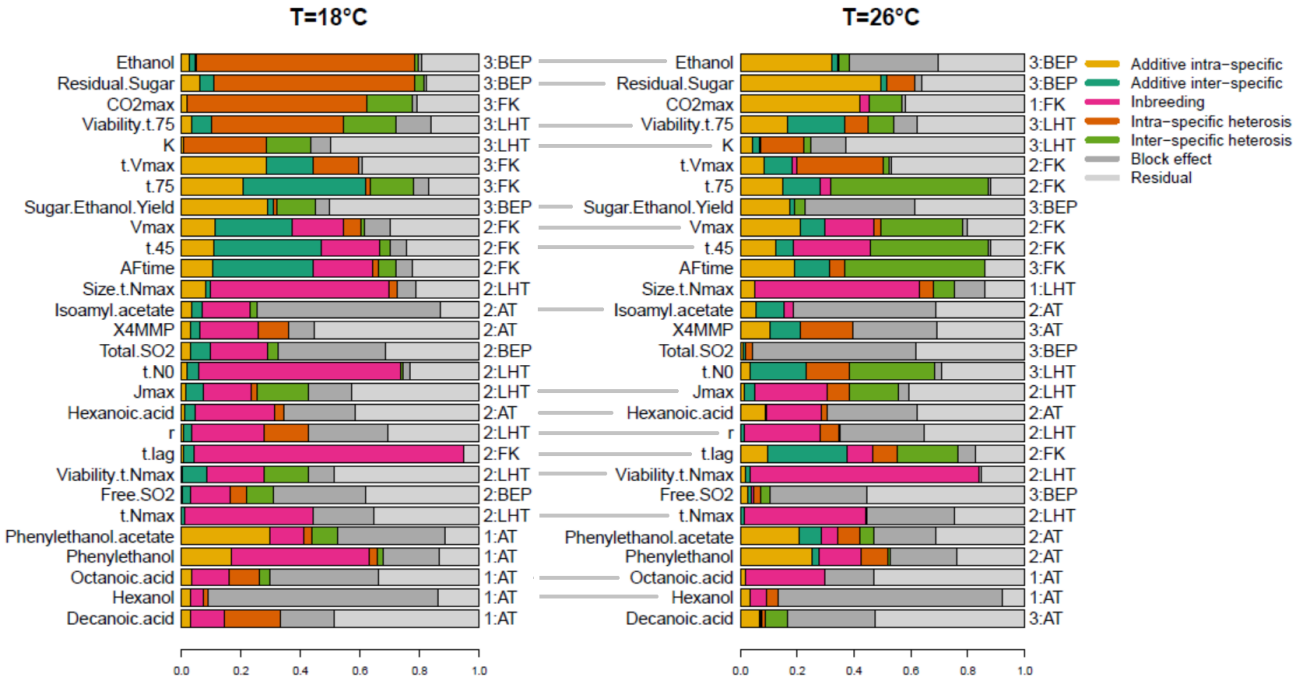

Figure SF8 Variance components of fermentation traits. **Left**: Traits measured at 18°C. **Right**: Traits measured at 26°C. Each variance component is attributed a different color. Traits are ranked according to their cluster number at 18°C. Trait category and cluster number is indicated on the right-hand-side of the plot.

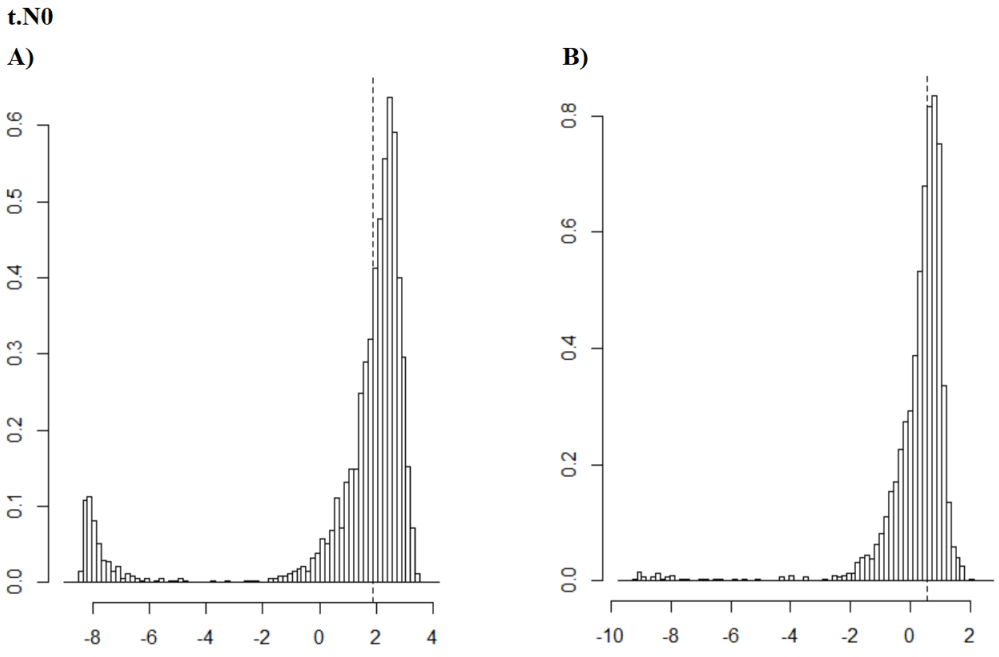

Figure SF9 Bootstrap summary example: Distribution of intra-specific variance estimates for the growth lag-phase, *t.N0*, at **A)** 18° and **B)** 26°C.

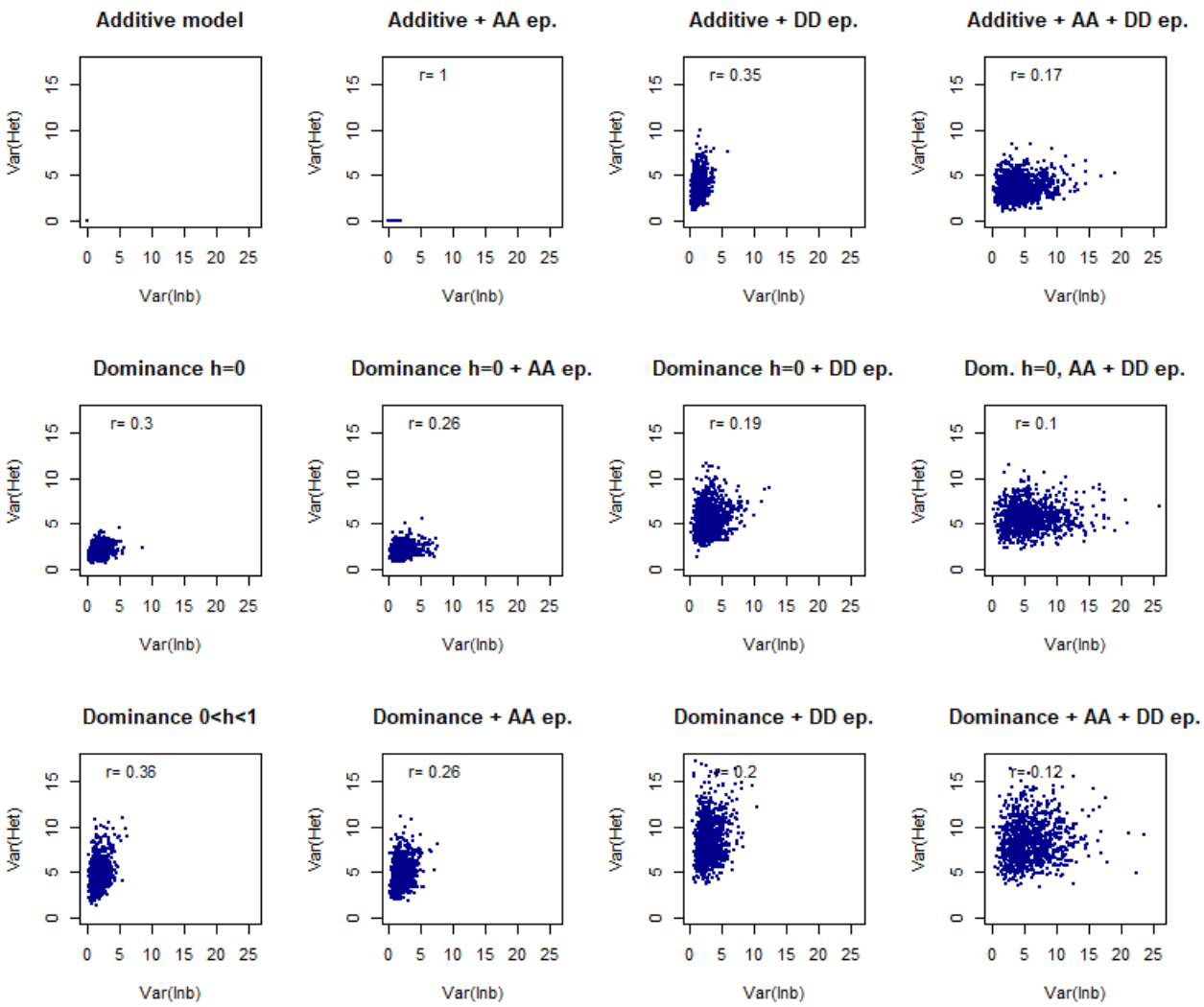

Figure SF10 Simulations genetic models. Correlation between inbreeding and heterosis variance computed on the basis of a combination of multilocus genetic models: Additive model with/without additive by additive, dominance by dominance, or both epistatic effects, dominance of the strongest allele with/without additive by additive, dominance by dominance, or both epistatic effects; symmetrical dominance with/without additive by additive, dominance by dominance, or both epistatic effects. The simulated half-diallel consisted of 11 parental lines. Phenotypic values were supposed to depend on 10 loci, and the number of alleles per loci was imposed to 11. Alleles values were drawn from a gamma distribution (k=10, θ=20) and epistatic effects from a normal distribution ($\mathcal{N}(0,3)$).

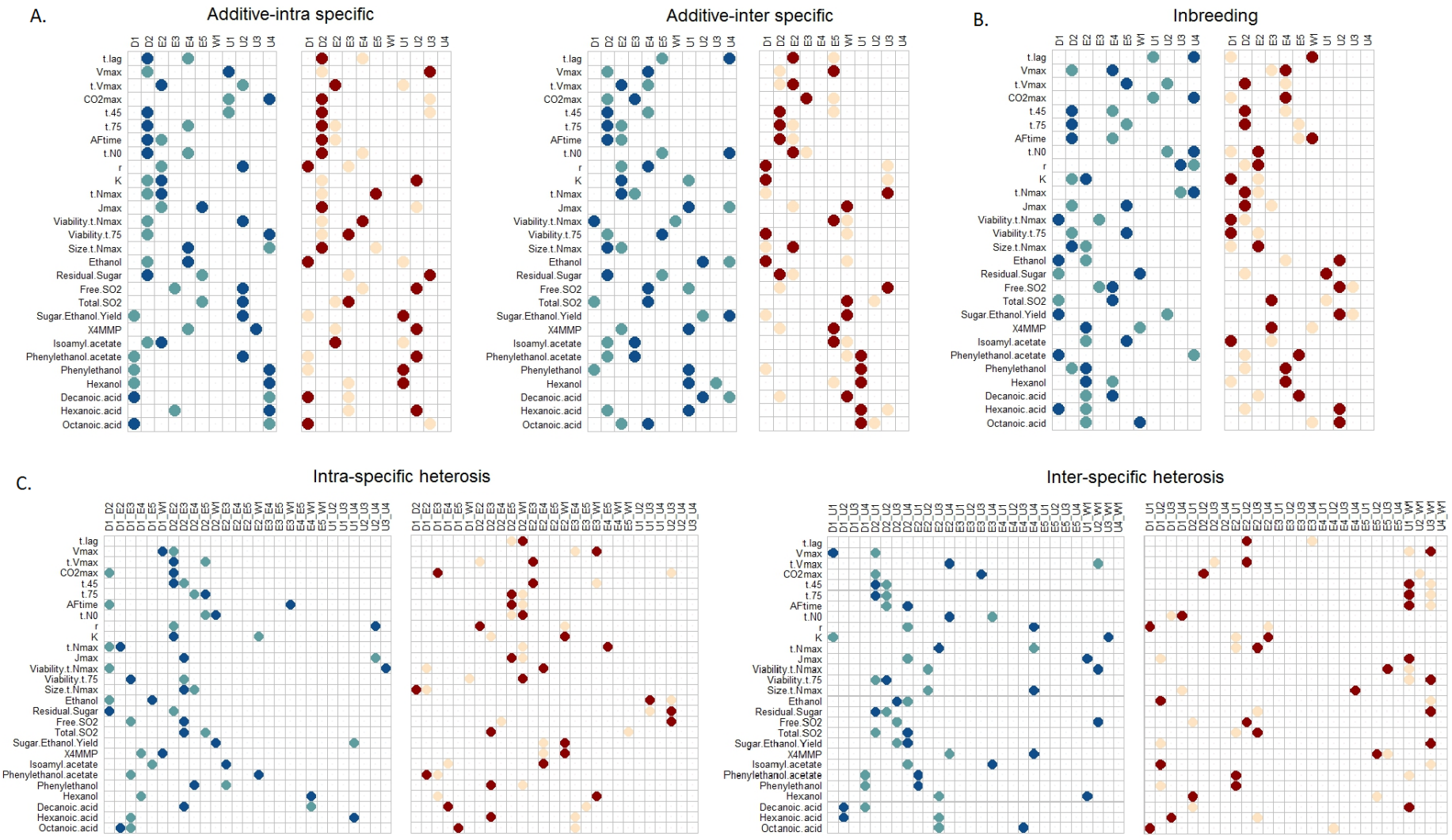

Figure SF11 Dots show strains with highest and lowest genetic contribution per trait and temperature, in blue at 18°C and in red at 26°C. Dark and light colors report the strains with the highest and lowest additive (A), inbreeding (B) and heterosis (C) contributions, respectively. Strains are sorted by species and traits by category.

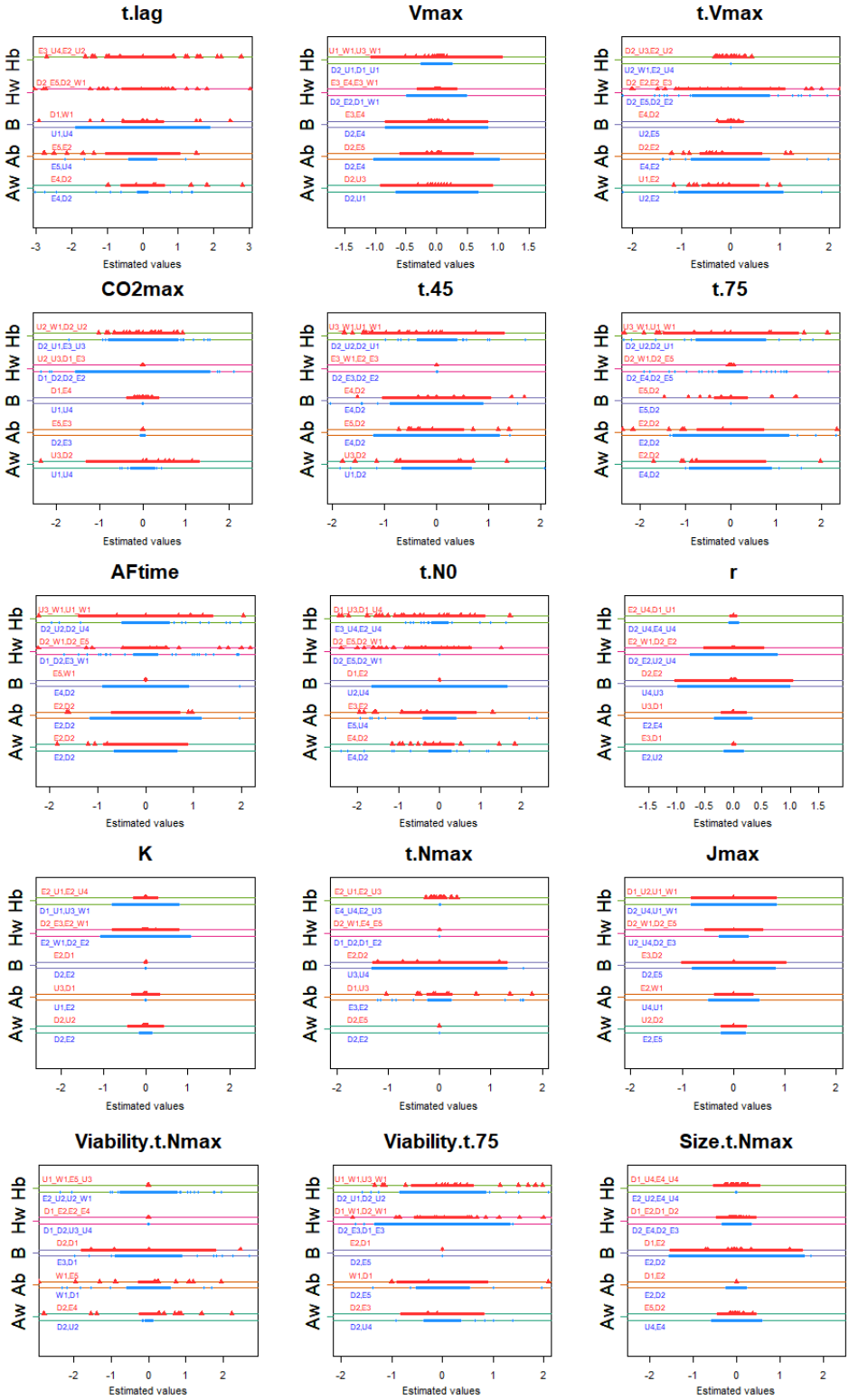
t.lag
Vmax
t.Vmax
CO2max
t.45
t.75
AFtime
t.N0
r
K
t.Nmax
Jmax
Viability.t.Nmax
Viability.t.75
Size.t.Nmax
Aw Ab B Hw Hb
Estimated values

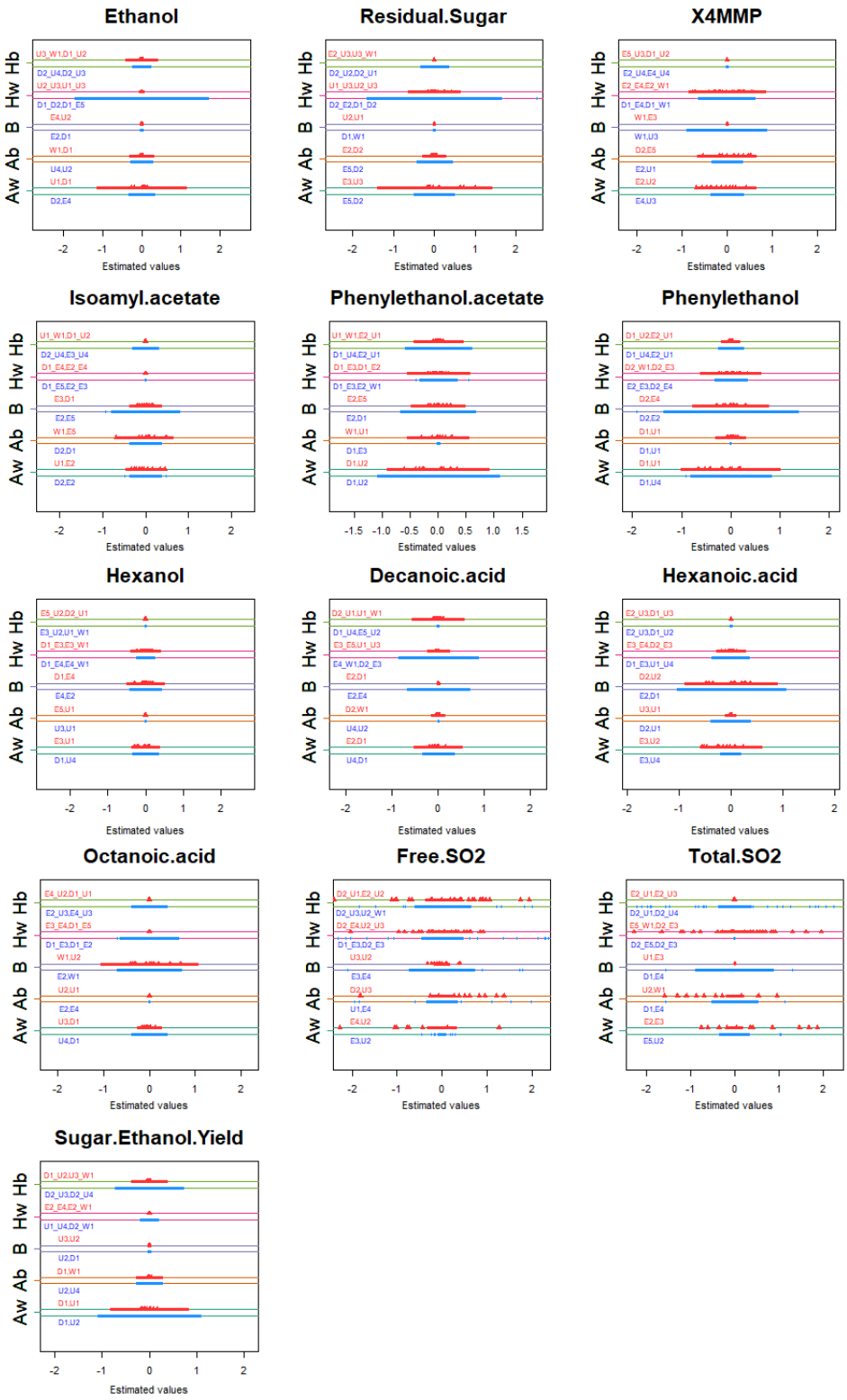

Figure SF12 Interval plots. For each fermentation and life-history trait we plot the Best Linear Unbiased Predictors of the random genetic effects estimated through the decomposition of our diallel design. The random genetic effect estimates, namely $\hat{A}_w$, $\hat{A}_b$, $\hat{B}$, $\hat{H}_w$, $\hat{H}_b$ are plotted in blue (18°C), or in red (26°C). Horizontal bars are added to show, for each parameter, the region of highest density that covers nearly 95% ($\sim \pm 2\hat{\sigma}_q$) of the parameter density. On the left hand-side of each plot we list, for each genetic effect, the strains which have the lowest and the greatest value of the respective genetic effect. The plot shows that: (i) genetic effects differ in a large extent between the two temperatures; (ii) additive and heterosis effects depend on the type of cross in which a line is involved (intra- or inter-specific); (iii) for some traits, genetic variances are strongly influenced by a particular hybrid combination.